

# Paleoceanography and Paleoclimatology

## RESEARCH ARTICLE

10.1029/2020PA003876

### Key Points:

- The highest mid-depth negative  $\delta^{13}\text{C}$  excursions occurred in the western tropical South Atlantic and dissipated further south
- Reduced Northern Component Water ventilation in the western tropical South Atlantic mid-depth during Heinrich Stadials
- Decreased Northern Component Water  $\delta^{13}\text{C}$  source signal and accumulation of respired carbon drove mid-depth negative excursions in  $\delta^{13}\text{C}$

### Supporting Information:

- Supporting Information S1

### Correspondence to:

M. C. Campos,  
marilia.carvalho.campos@usp.br

### Citation:

Campos, M. C., Chiessi, C. M., Venancio, I. M., Pinho, T. M. L., Crivellari, S., Kuhnert, H., et al. (2020). Constraining millennial-scale changes in Northern Component Water ventilation in the western tropical South Atlantic. *Paleoceanography and Paleoclimatology*, 35, e2020PA003876. <https://doi.org/10.1029/2020PA003876>

Received 6 FEB 2020

Accepted 5 MAY 2020

Accepted article online 12 MAY 2020

## Constraining Millennial-Scale Changes in Northern Component Water Ventilation in the Western Tropical South Atlantic

Marília C. Campos<sup>1</sup> , Cristiano M. Chiessi<sup>1</sup> , Igor M. Venancio<sup>2</sup> , Tainá M.L. Pinho<sup>3</sup> , Stefano Crivellari<sup>3</sup> , Henning Kuhnert<sup>4</sup> , Gerhard Schmiedl<sup>5</sup> , Rut A. Díaz<sup>6</sup> , Ana Luiza S. Albuquerque<sup>6</sup> , Rodrigo C. Portilho-Ramos<sup>4</sup> , André Bahr<sup>7</sup> , and Stefan Mulitza<sup>4</sup> 

<sup>1</sup>School of Arts, Sciences and Humanities, University of São Paulo, São Paulo, Brazil, <sup>2</sup>Center for Weather Forecasting and Climate Studies (CPTEC), National Institute for Space Research (INPE), Cachoeira Paulista, Brazil, <sup>3</sup>Institute of Geosciences, University of São Paulo, São Paulo, Brazil, <sup>4</sup>MARUM—Center for Marine Environmental Sciences, University of Bremen, Bremen, Germany, <sup>5</sup>Center for Earth System Research and Sustainability, Institute for Geology, University of Hamburg, Hamburg, Germany, <sup>6</sup>Graduate Program in Geochemistry, Fluminense Federal University, Niterói, Brazil, <sup>7</sup>Institute of Earth Sciences, Heidelberg University, Heidelberg, Germany

**Abstract** Negative excursions in the stable carbon isotopic composition ( $\delta^{13}\text{C}$ ) at Atlantic intermediate to mid-depths are common features of millennial-scale events named Heinrich Stadials. The mechanisms behind these excursions are not yet fully understood, but most hypotheses agree on the central role played by the weakening of the Atlantic meridional overturning circulation. Marine records registering millennial-scale negative  $\delta^{13}\text{C}$  excursions in the Atlantic are mostly restricted to the Heinrich Stadials of the last deglacial, while the Heinrich Stadials of the last glacial are poorly studied. Here, we constrain changes in bottom water ventilation in the western tropical South Atlantic mid-depth during Heinrich Stadials of the last glacial and deglacial by investigating marine core M125-95-3. The concurrent decreases in benthic foraminifera  $\delta^{13}\text{C}$  and increases in bulk sediment sulfur indicate an increased Northern Component Water (NCW) residence time in the western tropical South Atlantic mid-depth during Heinrich Stadials. Furthermore, a coherent meridional pattern emerges from the comparison of our new data to previously published mid-depth records from the western South Atlantic. While our record shows the largest negative  $\delta^{13}\text{C}$  excursions during almost all Heinrich Stadials, the western equatorial Atlantic showed medium and the subtropical South Atlantic showed the smallest negative excursions. This meridional pattern supports the notion that during Heinrich Stadials, a reduction in the NCW  $\delta^{13}\text{C}$  source signal together with the accumulation of respired carbon at NCW depths drove the negative  $\delta^{13}\text{C}$  excursions. We suggest that the negative  $\delta^{13}\text{C}$  excursions progressively increase along the NCW southwards pathway until the signal dissipates/dilutes by mixing with Southern Component Water.

## 1. Introduction

Negative excursions in the reconstructed stable carbon isotopic composition of dissolved inorganic carbon ( $\delta^{13}\text{C}_{\text{DIC}}$ ) at Atlantic intermediate (here, 1,000–1,500 m) to mid-depths (here, 1,500–2,500 m) have been reported to occur during millennial-scale climate change events named Heinrich Stadials. These excursions are often related to a reduced Atlantic meridional overturning circulation (AMOC) (Lund et al., 2015; Oppo et al., 2015; Oppo & Fairbanks, 1987; Tessin & Lund, 2013; Voigt et al., 2017). The reduced AMOC is frequently associated with (i) changes in the proportion of Northern Component Water (NCW) relative to Southern Component Water (SCW) (Keigwin & Lehman, 1994; Zahn et al., 1997), (ii) a shallow boundary between NCW and SCW (Curry et al., 1999; Meckler et al., 2013), and/or (iii) a decrease in the NCW  $\delta^{13}\text{C}$  source value (Lund et al., 2015; Oppo et al., 2015; Voigt et al., 2017). Additionally, increasing evidence suggests that the accumulation of respired carbon ( $^{12}\text{C}$  enriched) in the ocean interior in response to increased deep water residence time also contributed to the  $\delta^{13}\text{C}$  decreases in the Atlantic during these events (Oppo et al., 2015; Schmittner & Lund, 2015; Voigt et al., 2017). However, the exact mechanisms responsible for the negative  $\delta^{13}\text{C}$  excursions during millennial-scale events remain elusive. Furthermore, most Atlantic

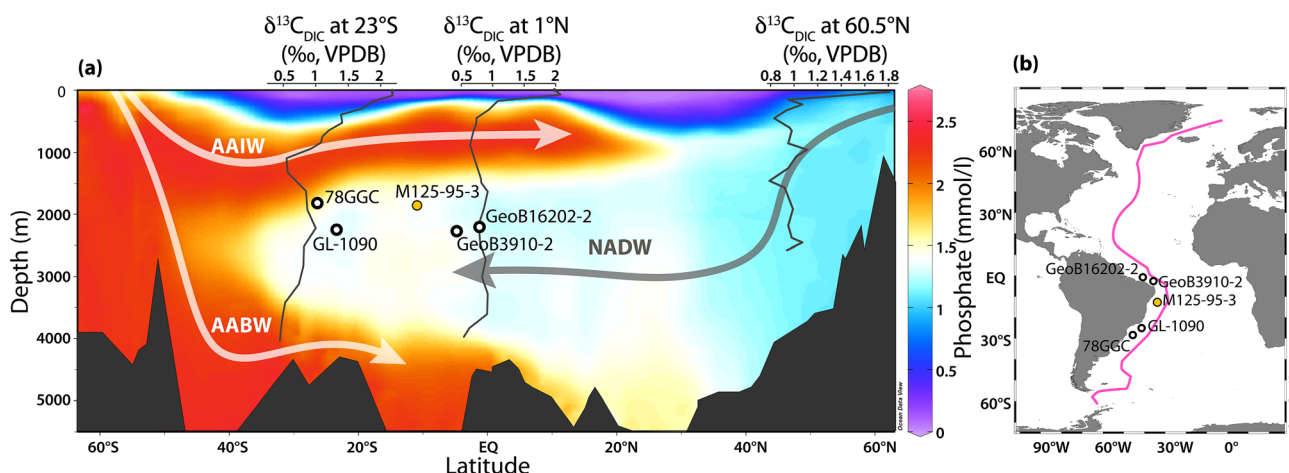


**Figure 1.** Location of core M125-95-3 (yellow filled dot) and other marine records discussed herein (open dots) (see details in Table 1). (a) Modern western Atlantic WOA13 phosphate section depicts the main water masses within the western Atlantic (Garcia et al., 2013) together with three vertical GEOSECS stable carbon isotopic composition profiles of dissolved inorganic carbon ( $\delta^{13}\text{C}_{\text{DIC}}$ ) at 60.5°N, 1°N, and 23°S (Kroopnick, 1985). Schematic arrows show the flow direction of the main water masses. AABW = Antarctic Bottom Water; AAIW = Antarctic Intermediate Water; NADW = North Atlantic Deep Water. (b) Location of western South Atlantic marine sediment cores. The purple line marks the section depicted in (a). This figure was partially produced with Ocean Data View (Schlitzer, 2018).

paleoclimate records registering negative excursions during Heinrich Stadials only cover the last deglacial Heinrich Stadials (i.e., Heinrich Stadial 1 and the Younger Dryas [YD]), while records spanning the Heinrich Stadials of the last glacial (i.e., from Heinrich Stadial 6 to 2) with appropriate temporal resolution are scarce (e.g., Burckel et al., 2015; Santos et al., 2017).

Here, we investigate marine sediment core M125-95-3 collected at the western tropical South Atlantic mid-depth (10.94°S, 1,897 m) spanning the last ca. 70 thousand years (ka). The high temporal resolution of this core allows us to constrain changes in bottom water conditions during Heinrich Stadials. To reconstruct past changes in the  $\delta^{13}\text{C}_{\text{DIC}}$ , we measured benthic foraminifera  $\delta^{13}\text{C}$ . In addition, to independently assess past changes in bottom water ventilation and the related changes in the accumulation of respiration carbon, we measured bulk sediment sulfur (S) content. Our  $\delta^{13}\text{C}$  data constitute the first record in the western South Atlantic that clearly registers all Heinrich Stadials of the last glacial and deglacial (i.e., from Heinrich Stadial 6 to the YD). The coeval decreases in  $\delta^{13}\text{C}$  and increases in S during Heinrich Stadials indicate a longer NCW residence time and accumulation of respiration carbon in the western tropical South Atlantic mid-depth.

## 2. Background

The western South Atlantic is occupied by a NCW that is, in turn, enveloped by two SCW. The NCW North Atlantic Deep Water (NADW) occurs between ~1,200 and 4,000 m water depth, whereas the SCW Antarctic Intermediate Water (AAIW) and Antarctic Bottom Water (AABW) occur above and below NADW, respectively (Figure 1a) (Stramma & England, 1999).

The distribution of  $\delta^{13}\text{C}_{\text{DIC}}$  within the oceans results from a complex combination of surface primary productivity, organic matter remineralization in greater depths, air-sea gas exchanges, and their interactions with ocean circulation (Figure 1a) (Kroopnick, 1985; Sarmiento et al., 1988). While the surface primary productivity preferentially removes nutrients and  $^{12}\text{C}$  from upper waters, the remineralization (or respiration) of organic matter returns nutrients and  $^{12}\text{C}$  to intermediate-deep waters (Figure 1a) (Sarmiento et al., 1988). As a result, nutrients and  $\delta^{13}\text{C}_{\text{DIC}}$  have an inverse relationship (Kroopnick, 1985). Newly formed deep water masses containing high fraction of oligotrophic surface waters (e.g., NADW) have relatively low nutrient content (i.e., low preformed nutrient) and respiration carbon, resulting in high  $\delta^{13}\text{C}_{\text{DIC}}$  (~1‰, Figure 1a— $\delta^{13}\text{C}_{\text{DIC}}$  vertical profile at 60.5°N) (Kroopnick, 1985). These high  $\delta^{13}\text{C}_{\text{DIC}}$  values spread into the deep North Atlantic. However, the aging effect and the accumulation of respiration carbon along the NCW pathway southwards promote a slight and progressive decrease in its  $\delta^{13}\text{C}_{\text{DIC}}$  signature (~0.9‰, Figure 1a— $\delta^{13}\text{C}_{\text{DIC}}$  vertical profile at

**Table 1**  
*Marine Sediment Cores Discussed in This Study*

Core ID	Region	Latitude (°S)	Longitude (°W)	Water depth (m)	Reference
GeoB16202-2	Western equatorial Atlantic	1.91	41.59	2,248	Voigt et al. (2017)
GeoB3910-2	Western equatorial Atlantic	4.25	36.35	2,362	Burckel et al. (2015)
M125-95-3	Western tropical South Atlantic	10.94	36.20	1,897	This study
GL-1090	Western subtropical South Atlantic	24.92	42.51	2,225	Santos et al. (2017)
78GGC	Western subtropical South Atlantic	27.48	46.33	1,820	Tessin and Lund (2013)

1°N). SCW, on the other hand, originate from waters with relatively high nutrients and respiration carbon and, thus, lower  $\delta^{13}\text{C}_{\text{DIC}}$  values spread northwards at AAIW (~0.5‰) and AABW (~0.4‰) levels (Kroopnick, 1985) (Figure 1a— $\delta^{13}\text{C}_{\text{DIC}}$  vertical profile at 23°S). As the water mass residence time increases, nutrients and respiration carbon become more concentrated, producing lower  $\delta^{13}\text{C}_{\text{DIC}}$  signatures. Since the residence time of western Atlantic deep waters is relatively short (ca. 275 years) (Stuiver et al., 1983), its  $\delta^{13}\text{C}_{\text{DIC}}$  may reflect the mixing of water masses of different initial  $\delta^{13}\text{C}_{\text{DIC}}$  values (i.e., NCW and SCW) and thus be a tracer for deep water mass structure and circulation (Kroopnick, 1985; Oppo & Fairbanks, 1987). Importantly, the  $\delta^{13}\text{C}_{\text{DIC}}$  may also be influenced by local processes like changes in surface primary productivity (e.g., in upwelling regions) and the related phytoplankton flux to the seafloor, as well as by the terrigenous input of low  $\delta^{13}\text{C}$  detritus (e.g., by riverine input) (Mackensen et al., 1993; Theodor et al., 2016).

The stable oxygen isotopic composition of seawater ( $\delta^{18}\text{O}_{\text{sw}}$ ) is also a potential tracer for water mass structure and circulation (LeGrande & Schmidt, 2006). Water masses have different  $\delta^{18}\text{O}_{\text{sw}}$  signatures that are dependent on their formation conditions. Assuming negligible geothermal and pressure heating effects, bottom water  $\delta^{18}\text{O}$  can only change due to mixing between water masses and thus is a valuable water mass tracer (e.g., Meredith et al., 1999). It is noteworthy that absolute  $\delta^{18}\text{O}_{\text{sw}}$  values are also influenced by global ice volume (e.g., Schrag et al., 2002). This effect is, however, nearly synchronous in specific ocean basins and water depths (Waelbroeck et al., 2011).

Since the presence of S in marine sediments is related to oxygen availability (i.e., redox conditions), changes in S concentration at seafloor sediments can, together with other proxies, record changes in local bottom water ventilation. Organic matter in marine sediments is degraded by different terminal electron acceptors encompassing aerobic and anaerobic degradation (Jørgensen et al., 2019). When oxygen availability is reduced, seawater sulfate ( $\text{SO}_4^{2-}$ ) becomes the dominant terminal electron acceptor. In this situation, organic matter degradation is performed by sulfate-reducing bacteria, and both pyrite and sulfurized organic matter are the results of the sulfate reduction and the main sinks of S at the seafloor (Jørgensen & Kasten, 2006; Suits & Arthur, 2000). Importantly, in regions where the local flux of organic carbon exported to the seafloor is low through time (e.g., far from upwelling systems and without river-borne nutrient input), the increase in S concentration may be related to an increase in bottom water residence time and in the accumulation of respiration carbon.

Here, we use species-specific benthic foraminifera  $\delta^{13}\text{C}$  and  $\delta^{18}\text{O}$  as well as the S content of bulk sediments to assess changes in bottom waters in the mid-depth western tropical South Atlantic.

### 3. Material and Methods

#### 3.1. Marine Sediment Core

Core M125-95-3 (10.94°S, 36.20°W, 1,897 m water depth, 10.4 m core length) was collected from the continental slope in the western tropical South Atlantic during R/V Meteor cruise M125 (Table 1) (Bahr et al., 2016). The core site is presently bathed in NADW (Figure 1a). Since we focus here on the Heinrich Stadials of the last glacial and deglacial (i.e., Marine Isotope Stages [MIS] 4, 3, and 2), we analyzed the uppermost ~7.4 m of the core. This section was sampled with syringes of 10 cm<sup>3</sup> and u-channels (2 cm width, 2 cm depth, and 105 cm length). Samples for isotopic and micropaleontological analyses were wet sieved and oven dried at 50 °C, and the fraction larger than 125 µm was stored in glass vials. Samples for bulk sediment analyses were stored at 4 °C.

We discuss our records in the context of four other published marine sediment cores also collected at the western South Atlantic mid-depth spanning from 1.91°S to 27.48°S (Table 1 and Figure 1). Cores GeoB3910-2 (Burckel et al., 2015) and GL-1090 (Santos et al., 2017) cover most Heinrich Stadials of the last glacial. In order to complement GeoB3910-2 upper portion and to improve the temporal resolution of GL-1090 during Heinrich Stadial 1 and the YD, we also compiled cores GeoB16202-2 (Voigt et al., 2017) and 79GGC (Tessin & Lund, 2013), which cover the last ~20 ka (Figures 3d, 3e, 3g, and 3h). We focus on mid-depth (around 2,000 m) and on the western margin of the Atlantic because this region is occupied by the Deep Western Boundary Current, being ideal for tracking past changes in NCW (Rhein et al., 1995).

### 3.2. Stable Isotopic Composition of Benthic Foraminifera

$\delta^{13}\text{C}$  and  $\delta^{18}\text{O}$  analyses were performed on two benthic foraminifera species with different microhabitat (McCorkle et al., 1990): (i) shallow infaunal species *Uvigerina* spp. (mainly *Uvigerina peregrina*;  $\delta^{18}\text{O}$  results previously published in Campos et al., 2019) and (ii) epifaunal species *Cibicidoides pachyderma*. From the sediment fraction larger than 125  $\mu\text{m}$ , ~3–10 specimens per sample were handpicked under a binocular microscope every 4–6 cm for *Uvigerina* spp. and every 2–50 cm for *C. pachyderma*. Since *C. pachyderma* (and also any other appropriate epibenthic species) is not consistently present in core M125-95-3, we only analyzed the depth interval 84–398 cm. On the other hand, *Uvigerina* spp. is present in the whole investigated section and was used to produce the main downcore  $\delta^{13}\text{C}$  record of M125-95-3. *Uvigerina* spp. analyses were conducted with a gas isotope ratio mass spectrometer (Thermo Fisher Scientific MAT253plus) coupled to an automated carbonate preparation device (Kiel IV) at the MARUM—Center for Marine Environmental Sciences, University of Bremen, Germany. *C. pachyderma* analyses were conducted with a gas isotope ratio mass spectrometer (Thermo Fisher Scientific MAT253) coupled to an automated carbonate preparation device (Kiel IV) at the Paleoceanography and Paleoclimatology Laboratory (P2L), University of São Paulo, Brazil. Output data were calibrated against in-house standard (both laboratories use Solnhofen Limestone) that is calibrated against the NBS19 standard. We report the results in per mil (parts per thousand, i.e., ‰) versus Vienna PeeDee belemnite (VPDB). For the measured period, the standard deviation of in-house standard replicate measurements was 0.03‰ ( $\delta^{13}\text{C}$ ) for both laboratories and 0.06‰ ( $\delta^{18}\text{O}$ ) for the MARUM and 0.05‰ for the P2L.

Benthic foraminifera register in their tests local bottom or pore water conditions, depending on the species-specific microhabitat and vital effects related to isotopic fractionation during biomineralization. Thus, their  $\delta^{13}\text{C}$  and  $\delta^{18}\text{O}$  have been widely used to reconstruct past changes in the local bottom water  $\delta^{13}\text{C}_{\text{DIC}}$  (Mackensen et al., 1993; Mackensen & Schmiedl, 2019; McCorkle et al., 1990) and  $\delta^{18}\text{O}_{\text{sw}}$  (Skinner & Shackleton, 2005; Waelbroeck et al., 2002; Waelbroeck et al., 2011). In order to directly compare our *Uvigerina* spp.  $\delta^{13}\text{C}$  values to the  $\delta^{13}\text{C}$  of epifaunal species, we applied the correction factor (0.9‰) from Shackleton and Hall (1984).

### 3.3. Sulfur Content

S intensity was determined with an X-ray fluorescence (XRF) core scanner and an energy-dispersive polarized XRF (EDP-XRF). XRF core scanner S data were collected every 5 mm downcore directly at the surface of u-channels sampled from the archive half of core M125-95-3. Analyses were performed at the MARUM—Center for Marine Environmental Sciences, University of Bremen, Germany, with the XRF Core Scanner III (AVAAATECH Serial No. 12) (details regarding the method are provided in Campos et al., 2019). EDP-XRF S analyses were performed on bulk sediment samples every 20 cm of the working half of core M125-95-3. Bulk sediment samples of around 10  $\text{cm}^3$  were freeze dried and homogenized with a hand agate mortar and pestle. Analyses were performed at the Oceanography and Paleoceanography Laboratory (LOOP), Fluminense Federal University, Brazil, with an energy-dispersive PANalytical Epsilon 3-X XRF spectrometer.

In marine sediments, organic matter is degraded by different terminal electron acceptors following an order of decreasing energy yield (from high to low values): oxygen, nitrate, oxides of manganese (IV) and iron (III), and sulfate (Jørgensen et al., 2019). Under oxygen depletion, the sulfate ( $\text{SO}_4^{2-}$ )—which is highly concentrated (~28 mM) in seawater—turns the dominant terminal electron acceptor, despite the others to be energetically more favorable. Where ventilation is reduced, organic matter starts to be degraded by sulfate-reducing bacteria (degradation/anaerobic respiration of organic matter). During this process, the

dissolved sulfate suffers reduction to sulfide ( $\text{H}_2\text{S} + \text{HS}^- + \text{S}^{2-}$ ) (e.g., Jørgensen & Kasten, 2006; Suits & Arthur, 2000). The produced sulfide can react with ferrous iron (provided by chemical reduction of detrital minerals) forming pyrite. In another diagenetic pathway, the produced sulfide can react with organic matter to form organic S compounds (i.e., sulfurization of organic matter) (Bottrell & Newton, 2006; Jørgensen et al., 2019). Both pyrite and sulfurized organic matter are the main sinks of S in marine sediments.

### 3.4. Foraminiferal Assemblages

Planktonic foraminifera assemblage analyses and total benthic foraminifera counts were conducted every ~10 cm of core M125-95-3. Samples were dry sieved with a 150  $\mu\text{m}$  mesh, and the species relative abundances were quantified from splits containing at least 300 specimens (Patterson & Fishbein, 1989). Taxonomy was based on Stainforth et al. (1975), Boltovskoy et al. (1980), and Bolli et al. (1989). Additionally, we counted the *Uvigerina* spp. abundance in nine samples of core M125-95-3 within the depth interval 212–282 cm, covering pre-Heinrich Stadial 2, Heinrich Stadial 2, and post-Heinrich Stadial 2. Samples were dry sieved with a 150  $\mu\text{m}$  mesh, and the *Uvigerina* spp. relative abundance was quantified from splits containing at least ~100 benthic specimens (Boyle, 1990; Schmiedl et al., 2000). Taxonomy was based on Boltovskoy et al. (1980) and Lutze (1986). Considering the water depth (i.e., 1,897 m) of core M125-95-3 as well as the modern and glacial lysocline depths (Volbers & Henrich, 2004), we assume that the planktonic and benthic foraminifera faunal composition of core M125-95-3 was not influenced by dissolution.

We estimate changes in surface primary productivity based on the index  $R_{\text{HP/Planktonic}}$ , in which HP represents the sum of the abundance of the high productivity species *Globigerina bulloides*, *Neogloboquadrina dutertrei*, *Neogloboquadrina incompta*, and *Globigerinata glutinata* divided by the sum of all planktonic species (Portilho-Ramos et al., 2017). Also, we infer the local flux of organic carbon exported to the seafloor based on (i) the benthic foraminifera accumulation rate (BFAR) (Dias et al., 2018; Herguera & Berger, 1991) and (ii) the abundance of the food indicator *Uvigerina* spp. relative to the abundance of all benthic foraminifera, that is,  $R_{\text{Uvigerina spp./Benthics}}$  (Boyle, 1990; Koho et al., 2008; Schmiedl & Mackensen, 1997).

### 3.5. Age Model

The analyzed section of core M125-95-3 covers the last ca. 70 ka with a mean sedimentation rate of 11.9 cm/ka. The chronology was obtained by combining nine planktonic foraminifera accelerator mass spectrometry (AMS) radiocarbon ages (covering the uppermost 452 cm, i.e., ca. 40 ka before present [BP]) with three M125-95-3 *Uvigerina* spp.  $\delta^{18}\text{O}$  tie-points aligned to a benthic  $\delta^{18}\text{O}$  reference curve from Govin et al. (2014). We used the calibration curve IntCal13 (Reimer et al., 2013) with a variable simulated reservoir age from transient modeling experiments described in Butzin et al. (2017). The age modeling algorithm BACON v. 2.2 (Blaauw & Christen, 2011) was used within the software PaleoDataView v. 0.8.3.4 (Langner & Mulitza, 2019) for age-depth modeling. Further details regarding the age model are provided in Campos et al. (2019).

## 4. Results

*Uvigerina* spp.  $\delta^{13}\text{C}$  values range from  $-1.43\text{\textperthousand}$  to  $0.47\text{\textperthousand}$  (Figure 2g). The contrast between mean last glacial and Holocene values is  $\sim 0.7\text{\textperthousand}$ . Negative excursions (as large as  $0.92\text{\textperthousand}$ ) in the *Uvigerina* spp.  $\delta^{13}\text{C}$  record occurring during MIS4-1 are associated with Heinrich Stadials (i.e., from Heinrich Stadial 6 to the YD). Although the negative excursion associated with Heinrich Stadial 3 is also present, it is not as marked as the excursions associated with other Heinrich Stadials. Apart from the Heinrich Stadials excursions, another negative millennial-scale excursion occurs around 44 ka BP. *Uvigerina* spp.  $\delta^{18}\text{O}$  values vary from  $2.63\text{\textperthousand}$  to  $5.02\text{\textperthousand}$  (Figure 2i). The contrast between mean last glacial and Holocene values is  $\sim 1.4\text{\textperthousand}$ . During the last glacial (MIS4-3), relative low values are coeval with Heinrich Stadial 6 to 4. The last deglaciation shows sharp decreases at ca. 18.4 and 11.5 ka BP, coeval (within age model uncertainties) to Heinrich Stadial 1 and the YD. *C. pachyderma* isotopic values vary between  $-1.33\text{\textperthousand}$  and  $-0.22\text{\textperthousand}$  for  $\delta^{13}\text{C}$  and 4.22 and  $5.41\text{\textperthousand}$  for  $\delta^{18}\text{O}$  (Figures 2f and 2h). Negative excursions are also associated with Heinrich Stadials (i.e., from Heinrich Stadial 3 to 1) in both records (i.e.,  $\delta^{13}\text{C}$  and  $\delta^{18}\text{O}$ ).

Despite localized differences (e.g., during Heinrich Stadial 6), the  $\delta^{13}\text{C}$  (Figures 2f and 2g) and the XRF core scanner S (Figure 2d) records show an inverse relationship during Heinrich Stadials. Higher Heinrich

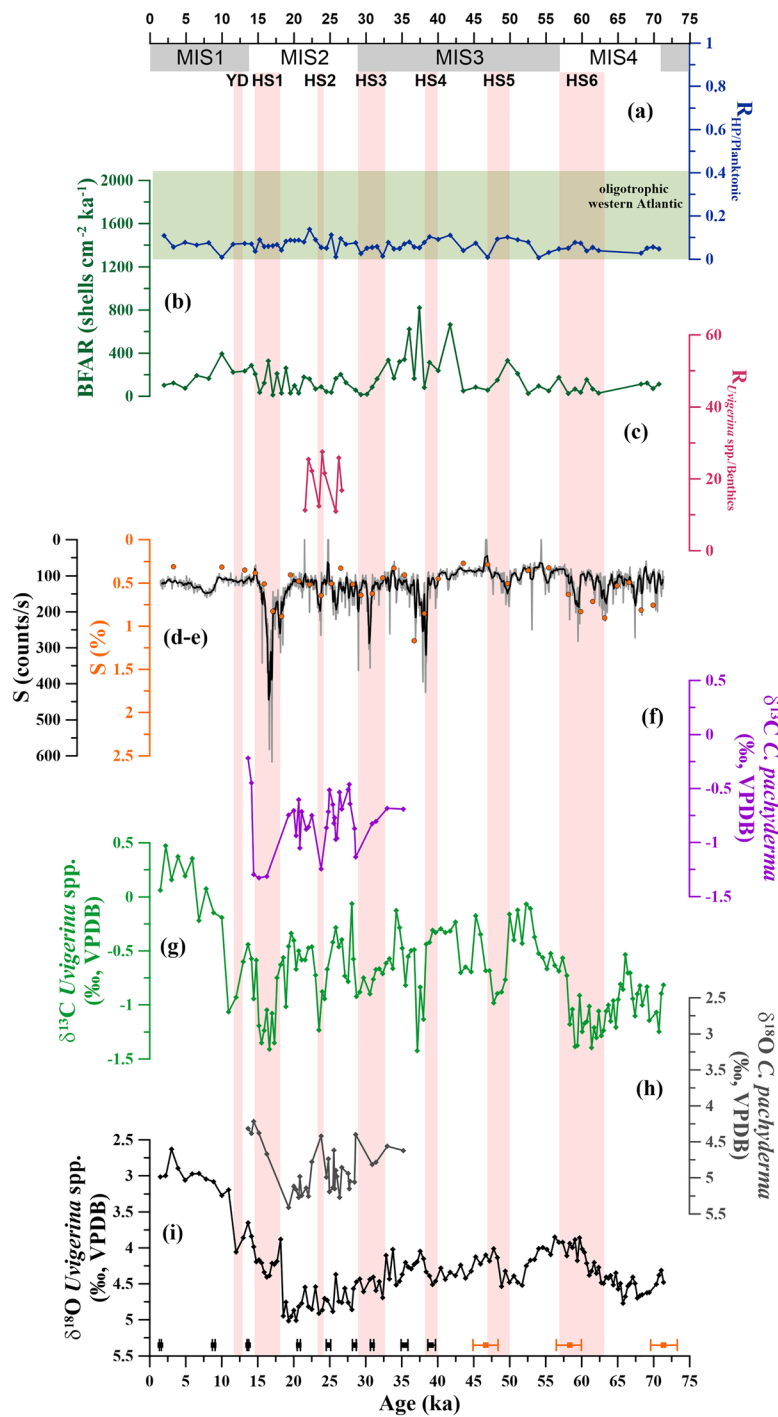


**Figure 2.** Isotopic, geochemical, and assemblage records from core M125-95-3 for the last ca. 70 ka. (a) Surface primary productivity index  $R_{HP}/\text{planktonic}$  (abundance of high productivity species [HP] divided by the abundance of all planktonic species). The green rectangle represents typical western Atlantic oligotrophic conditions (Garcia et al., 2013; Kucera et al., 2005); (b) benthic foraminifera accumulation rate (BFAR); (c) local flux of organic carbon to the seafloor index  $R_{Uvigerina \text{ spp.}/\text{Benthics}}$  (*Uvigerina* spp. abundance relative to at least  $\sim 100$  benthic specimens); (d, e) X-ray fluorescence (XRF) core scanner sulfur (S) (black line) and energy-dispersive polarized (EDP) XRF S (orange circles); (f) *Cibicidoides pachyderma* stable carbon isotopic composition ( $\delta^{13}\text{C}$ ); (g) *Uvigerina* spp.  $\delta^{13}\text{C}$ ; (h) *C. pachyderma* stable oxygen isotopic composition ( $\delta^{18}\text{O}$ ); and (i) *Uvigerina* spp.  $\delta^{18}\text{O}$  (previously published in Campos et al., 2019). Black (orange) squares at the bottom of the panel depict calibrated radiocarbon ages (tie-points) with  $2\sigma$  standard error. Red vertical bars represent millennial-scale events Younger Dryas (YD) and Heinrich Stadial (HS) 1 to 6. Marine Isotope Stages (MIS) are depicted below the upper axis.

Stadials XRF core scanner S intensities (i.e., from Heinrich Stadial 6 to the YD) interrupt the near-constant background (i.e., ~100 counts per second) present throughout the investigated interval. EDP-XRF S concentrations (Figure 2e) range from 0.27% to 1.17% and also show increases during most Heinrich Stadials (i.e., from Heinrich Stadial 6 to 1).

$R_{\text{HP/Planktonic}}$  values range from 0 to 0.14 (Figure 2a), being low throughout the last ca. 70 ka. BFAR values are also low during this period, varying from ~12 to 820 shells/cm<sup>2</sup>/ka (Figure 2b).  $R_{\text{Uvigerina spp./Benthics}}$  values vary between 10.96 to 27.55 (Figure 2c), showing no clear trend during the analyzed interval, that is, pre-Heinrich Stadial 2, Heinrich Stadial 2, and post-Heinrich Stadial 2.

## 5. Discussion

### 5.1. Benthic Foraminifera $\delta^{13}\text{C}$ Signal

The  $\delta^{13}\text{C}$  of epibenthic foraminifera is an optimal tracer for past changes in bottom water conditions (Mackensen & Schmiedl, 2019; McCorkle et al., 1990). The analyzed species *C. pachyderma* occupies an epifaunal to very shallow infaunal microhabitat (Fontanier et al., 2002; Schmiedl et al., 2000). Accordingly, the  $\delta^{13}\text{C}$  of *C. pachyderma* is close to bottom water  $\delta^{13}\text{C}_{\text{DIC}}$  with negligible pore water effects (Schmiedl et al., 2004; Theodor et al., 2016). In contrast, *Uvigerina* species commonly inhabit shallow infaunal microhabitats (e.g., Koho et al., 2008). Shallow infaunal benthic foraminifera calcify in contact with pore water, and their  $\delta^{13}\text{C}$  cannot be readily assumed to record  $\delta^{13}\text{C}_{\text{DIC}}$  of the overlying bottom water. Indeed, the  $\delta^{13}\text{C}_{\text{DIC}}$  of pore water is controlled by both (i) overlying bottom water  $\delta^{13}\text{C}_{\text{DIC}}$  and (ii) degradation of organic matter exported to the seafloor (e.g., from surface primary productivity and/or terrigenous input). The latter process leaves pore water  $^{12}\text{C}$ -enriched compared to overlying bottom water, thus affecting infaunal foraminifera  $\delta^{13}\text{C}$  (i.e., microhabitat effect) (McCorkle et al., 1985; McCorkle et al., 1990; Zahn et al., 1986). Our *Uvigerina* spp. negative  $\delta^{13}\text{C}$  excursions during Heinrich Stadials of the last glacial and deglacial (i.e., from Heinrich Stadial 6 to the YD; Figure 2g) could therefore be controlled by three possible processes (that could have operated together): (i) higher surface primary productivity (McCorkle et al., 1985); (ii) higher input and resuspension of low  $\delta^{13}\text{C}$  terrigenous detritus (Milzer et al., 2016; Polyak et al., 2003; Theodor et al., 2016); and (iii) changes in the overlying bottom water ventilation leading to lower  $\delta^{13}\text{C}_{\text{DIC}}$  (Voigt et al., 2017).

Our study area is far from upwelling systems, and it is dominated by oligotrophic western boundary currents (Garcia et al., 2013); thus, we would not expect to have increases in surface primary productivity. Indeed,  $R_{\text{HP/Planktonic}}$  show low values during the last ca. 70 ka, confirming that increases in surface primary productivity did not occur during Heinrich Stadials (Figure 2a). The low  $R_{\text{HP/Planktonic}}$  values also indicate that river-borne nutrients did not affect the upper water column of our core site during Heinrich Stadials (Schilman et al., 2001). Thus, changes in surface primary productivity cannot be the main driver of the negative  $\delta^{13}\text{C}$  excursions in our *Uvigerina* spp. record (Figure 2g).

Intervals of enhanced input of low  $\delta^{13}\text{C}$  terrigenous detritus could account for the negative excursions considering that our core site is located near the mouth of the São Francisco River and that increased input of terrigenous sediments (e.g., Ti and Fe) occurred during Heinrich Stadials (Campos et al., 2019). However, our low BFAR values during the last ca. 70 ka (Figure 2b) together with the lack of a clear trend in our  $R_{\text{Uvigerina spp./Benthics}}$  during the analyzed interval (i.e., pre-Heinrich Stadial 2, Heinrich Stadial 2, and post-Heinrich Stadial 2) (Figure 2c) suggest that the negative  $\delta^{13}\text{C}$  excursions were not accompanied by a marked increase in the local flux of organic carbon to the seafloor (Boyle, 1990; Theodor et al., 2016). Thus, we deem the input of low  $\delta^{13}\text{C}$  terrigenous detritus not to be the main driver of the negative  $\delta^{13}\text{C}$  excursions in our *Uvigerina* spp. record (Figure 2g).

Epibenthic *C. pachyderma*  $\delta^{13}\text{C}$  shows negative anomalies during Heinrich Stadial 3, 2, and 1 (Figure 2f), that is, all Heinrich Stadials covered by the *C. pachyderma* record. Importantly, the magnitudes of the *C. pachyderma* negative excursions are very similar to those of *Uvigerina* spp. (Figure 2g). This supports the suggestion that the local flux of organic carbon to the seafloor was indeed low having insignificant influence in our *Uvigerina* spp. negative  $\delta^{13}\text{C}$  excursions (Schmiedl & Mackensen, 2006; Theodor et al., 2016; Zahn et al., 1986). Taken together, we interpret the *Uvigerina* spp. negative excursions during all Heinrich Stadials of the last glacial and deglacial (Figure 2g) primarily as responses to changes in the overlying bottom water.

In the next section, we assess the possible changes that occurred in the overlying bottom water in the western South Atlantic mid-depth. We tentatively quantified the magnitude of the  $\delta^{13}\text{C}$  excursions present in our record as well as in records from four other cores collected at similar depths in the western South Atlantic (Table 1 and Figure 1). Therefore, we selected, whenever possible, the three more positive  $\delta^{13}\text{C}$  values of the preevents (i.e., intervals just before the respective negative excursion) and the three more negative  $\delta^{13}\text{C}$  values within the events (i.e., the negative excursions) (Figures 3d–3h) and calculated the magnitude of each excursion (i.e., pre-Heinrich Stadial  $\delta^{13}\text{C}$  minus Heinrich Stadial  $\delta^{13}\text{C}$ ). Because of age models uncertainties, the timing of Heinrich Stadials can be slightly different among the considered records.

## 5.2. Western Tropical South Atlantic Mid-depths Show the Largest Negative $\delta^{13}\text{C}$ Excursions During Heinrich Stadials

Atlantic depleted  $\delta^{13}\text{C}$  values at intermediate and mid-depths are commonly attributed to an increased fraction of low- $\delta^{13}\text{C}$  SCW (Boyle & Keigwin, 1987; Duplessy et al., 1988; Keigwin & Lehman, 1994; Sarnthein et al., 1994). A greater fraction of SCW AABW at our core site during Heinrich Stadials could have potentially contributed to the negative  $\delta^{13}\text{C}$  excursions (Figures 2g and 3f). Additionally, during these millennial-scale events, the relatively low- $\delta^{13}\text{C}$  SCW AABW source signal could have been overprinted by increased Southern Ocean air-sea gas exchange. An increase in Southern Ocean air-sea gas exchange during Heinrich Stadials is attributed to a reduced Southern Ocean stratification (Anderson et al., 2009) and a sea surface warming in the high latitudes of the Southern Hemisphere (EPICA, 2006; Lynch-Stieglitz et al., 1995). If this was the case (i.e., increased fraction of SCW AABW and/or depleted SCW AABW source signal), we would expect our  $\delta^{18}\text{O}$  values to increase since SCW AABW shows a relatively higher  $\delta^{18}\text{O}$  than NCW (LeGrande & Schmidt, 2006). However, they decrease during some Heinrich Stadials and present no clear trend during others (Figures 2h and 2i). It is noteworthy that the mentioned sea surface warming in the high latitudes of the Southern Hemisphere in response to a reduced AMOC (EPICA, 2006) would reduce the  $\delta^{18}\text{O}$  values of SCW AABW (Oppo et al., 2015). But it is unlikely that this process had a predominant influence at the bottom of the water column of our core site. Also, if a decreased SCW AABW  $\delta^{13}\text{C}$  source signal would have affected the bottom of the water column at our core site, we would expect the lowest mid-depth  $\delta^{13}\text{C}$  Heinrich Stadials excursions to occur to the south of our core site, what is not the case (see below). Mid-depth Atlantic water mass provenance records based on the neodymium isotopic composition of the authigenic fraction (a more robust proxy for water mass provenance than  $\delta^{18}\text{O}$ ) show that NCW dominated the depths around 2,000 m during Heinrich Stadials (Howe et al., 2018; Zhao et al., 2019).

Increased evidence suggest that the deglacial Atlantic negative  $\delta^{13}\text{C}$  excursions may be related to changes in NCW (Lund et al., 2015; Oppo et al., 2015; Schmittner & Lund, 2015; Voigt et al., 2017; Zhao et al., 2019). During events of weak AMOC (i.e., Heinrich Stadials), the reduced input of high  $\delta^{13}\text{C}$  surface waters into the deep North Atlantic due to decreased convection would promote a decrease in the source signal of the NCW (Lund et al., 2015; Oppo et al., 2015). Additionally, the reduced ventilation and consequent increased NCW residence time would have led to an increase in the accumulation of respired carbon at NCW depths throughout the Atlantic (Schmittner & Lund, 2015). Thus, the decreased NCW  $\delta^{13}\text{C}$  source signal during Heinrich Stadials was accentuated along the NCW pathway southwards by the accumulation of respired carbon. Proxies of water mass residence time and flow rates should confirm this scenario. In fact,  $^{14}\text{C}$ -depleted values (Chen et al., 2015; Lund et al., 2015; Robinson et al., 2005; Thornalley et al., 2011) and high sedimentary  $^{231}\text{Pa}/^{230}\text{Th}$  (Henry et al., 2016; McManus et al., 2004; Mulitza et al., 2017; Sükke et al., 2019) (Figures 3b and 3c) from the western Atlantic suggest a reduced ventilation at NCW depths coeval with freshwater input into the high latitudes of the North Atlantic (marked by pulses of ice-raftered debris [IRD]; Figure 3a).

Considering the progressive character of the  $\delta^{13}\text{C}$  decrease, we would expect the negative excursions to be smaller near the NCW source region, that is, reflecting almost exclusively the reduction in the NCW  $\delta^{13}\text{C}$  source signal, and the highest further south in the Atlantic, that is, reflecting a combination of reduced NCW  $\delta^{13}\text{C}$  source signal and accumulation of respired carbon at NCW depths. Then, the signal would dissipate/dilute by mixing with SCW (Lund et al., 2015; Schmittner & Lund, 2015; Tessin & Lund, 2013). Indeed, northern North Atlantic did not show markedly negative excursions during Heinrich Stadials (e.g., Elliot et al., 2002), and the largest  $\delta^{13}\text{C}$  negative excursion was reported to occur as far south as the western equatorial Atlantic intermediate depths ( $1.58^\circ\text{S}$ , 1,400 m) during Heinrich Stadial 1 (Voigt et al., 2017).

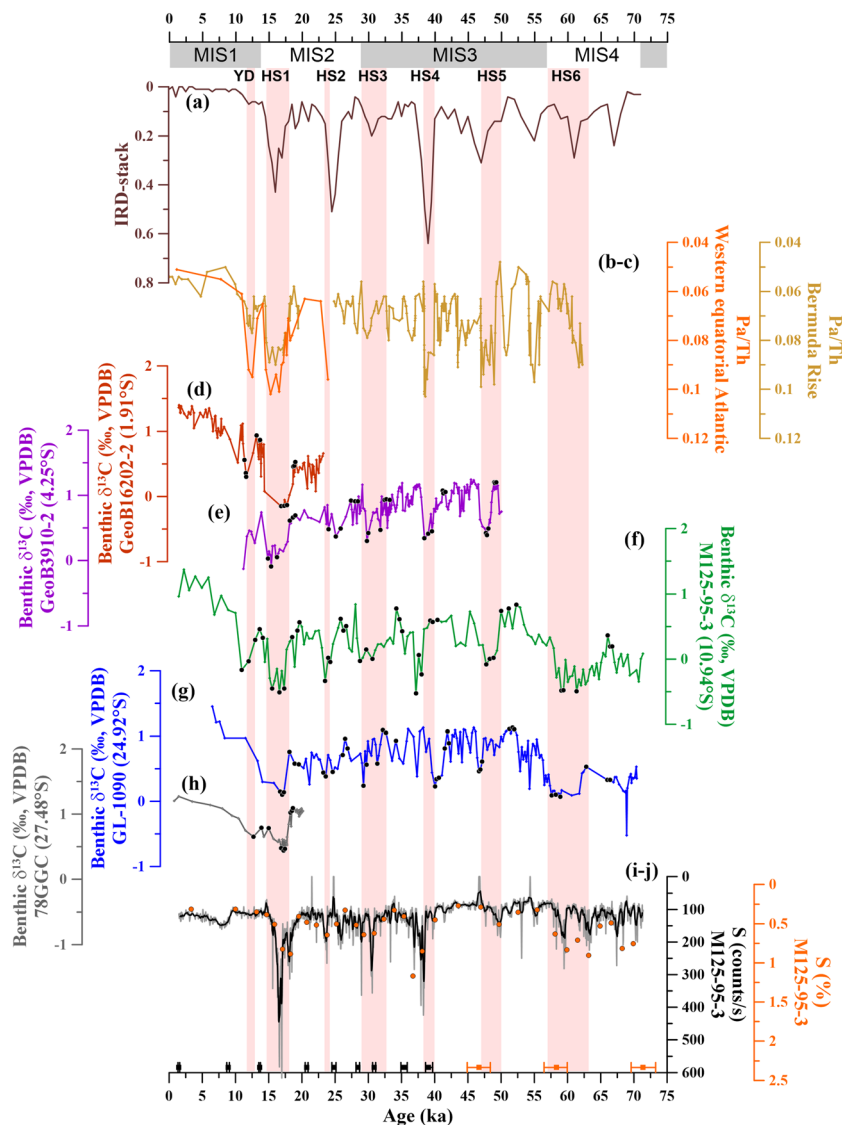


**Figure 3.** Paleoceanographic records from the Atlantic. (a) Heinrich layers indicated by the presence of ice-rafted debris (IRD) from the stack curve of Lisiecki and Stern (2016); (b) western equatorial Atlantic  $^{231}\text{Pa}/^{230}\text{Th}$  (Mulitza et al., 2017); (c) Bermuda Rise  $^{231}\text{Pa}/^{230}\text{Th}$  (Henry et al., 2016; McManus et al., 2004); (d) benthic (i.e., *Cibicides wuellerstorfi*, *Cibicidoides kullenbergi*, and *Cibicides lobatulus*) stable carbon isotopic composition ( $\delta^{13}\text{C}$ ) from core GeoB16202-2, western equatorial Atlantic (Voigt et al., 2017); (e) benthic (*C. wuellerstorfi*)  $\delta^{13}\text{C}$  from core GeoB3910-2, western equatorial Atlantic (Burckel et al., 2015); (f) benthic (i.e., *Uvigerina* spp. corrected for comparison to epibenthic species; correction factor based on Shackleton & Hall, 1984)  $\delta^{13}\text{C}$  from core M125-95-3, western tropical South Atlantic (this study); (g) benthic (i.e., *C. wuellerstorfi*)  $\delta^{13}\text{C}$  from core GL-1090, western subtropical South Atlantic (Santos et al., 2017); (h) benthic (i.e., *Cibicidoides* spp.)  $\delta^{13}\text{C}$  from core 78GGC, western subtropical South Atlantic (Tessin & Lund, 2013); and (i, j) X-ray fluorescence (XRF) core scanner sulfur (S) (black line) and energy-dispersive polarized (EDP) XRF S (orange circles) (this study). All benthic  $\delta^{13}\text{C}$  records (d)–(h) derived from mid-depth western South Atlantic cores ranging from 1,820 to 2,362 m water depth. Black filled circles in records (d)–(h) indicate the data points used to calculate the magnitude of the negative  $\delta^{13}\text{C}$  excursions (more details are found in Figure 4). Black (orange) squares at the bottom of the panel depict calibrated radiocarbon ages (tie-points) with  $2\sigma$  standard error. Red vertical bars represent millennial-scale events Younger Dryas (YD) and Heinrich Stadial (HS) 1 to 6. Marine Isotope Stages (MIS) are depicted below the upper axis.

However, most western South Atlantic marine records reporting negative excursions during Heinrich Stadials with appropriate temporal resolution only cover the last deglacial (i.e., Heinrich Stadial 1 and the YD), leaving aside the glacial Heinrich Stadials (i.e., Heinrich Stadial 6-2). Exceptions have been reported, so far, for two records from the western South Atlantic mid-depth, that is, GeoB3910-2 (4.25°S; Figure 3e) from the western equatorial Atlantic covering the interval ca. 50–11 ka (Burckel et al., 2015) and GL-1090 (24.92°S; Figure 3g) from the western subtropical South Atlantic covering the last ca. 185 ka (Santos

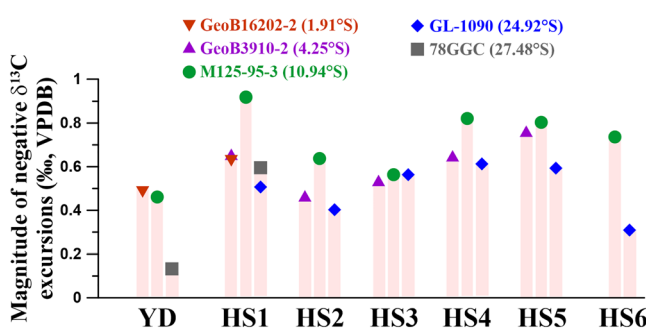


**Figure 4.** Heinrich Stadial (HS) magnitude of the negative  $\delta^{13}\text{C}$  excursions of western Atlantic cores (color coded according to Figure 3) GeoB16202-2 (equatorial Atlantic) (Voigt et al., 2017), GeoB3910-2 (equatorial Atlantic) (Burckel et al., 2015), M125-95-3 (tropical South Atlantic) (this study), GL-1090 (subtropical South Atlantic) (Santos et al., 2017), and 78GGC (subtropical South Atlantic) (Tessin & Lund, 2013). Excursions were calculated considering the three more positive values of the pre-Heinrich Stadials and the three more negative values of the Heinrich Stadials. The Younger Dryas (YD) and Heinrich Stadial 1 to 6 are depicted.

than Heinrich Stadials. Since our focus here relies on Heinrich Stadials, we do not further discuss this event. It is important to mention that MIS4 is characterized as a period of intense oceanic carbon sequestration (Bereiter et al., 2012) that could have overprinted the negative  $\delta^{13}\text{C}$  excursions during Heinrich Stadial 6 (Figures 3f and 3g).

The meridional pattern of negative  $\delta^{13}\text{C}$  excursions during most Heinrich Stadials supports the notion that the combined effect of (i) changes in the  $\delta^{13}\text{C}$  NCW source signal and (ii) the accumulation of respired carbon at mid-depth produced the largest negative  $\delta^{13}\text{C}$  excursions in the western tropical South Atlantic (i.e., M125-95-3 core site) from where it gradually lost magnitude by mixing with SCW until reaching the western subtropical South Atlantic (i.e., GL-1090 and 78GGC core sites) (Figure 5) (Lund et al., 2015; Schmittner & Lund, 2015; Tessin & Lund, 2013). Importantly, our independent proxy for bottom water

et al., 2017) (Table 1 and Figure 1). Our new  $\delta^{13}\text{C}$  record (Figure 3f) covers the last ca. 70 ka with a high temporal resolution, being ideal not only to constrain NCW ventilation in the western tropical South Atlantic mid-depth during Heinrich Stadials but also to fill the gap of marine records between 4.24°S and 24.92°S. Furthermore, core M125-95-3 provides the first western South Atlantic  $\delta^{13}\text{C}$  record that clearly registers all Heinrich Stadials of the last glacial and deglacial (i.e., from Heinrich Stadial 6 to the YD) (Lynch-Stieglitz et al., 2014).

The compilation of western South Atlantic mid-depth records together with our new record reveal the existence of a coherent meridional pattern of negative  $\delta^{13}\text{C}$  excursions during most Heinrich Stadials (Figures 3–5 and supporting information Figure S1). Core M125-95-3 shows systematically larger  $\delta^{13}\text{C}$  negative excursions, exception made for Heinrich Stadial 3 in which core GL-1090 shows the same magnitude of M125-95-3 and the YD in which core GeoB16202-2 shows a slightly higher magnitude (Figure 4). The negative  $\delta^{13}\text{C}$  excursion around 44 ka BP that can be seen in our record and in GeoB3910-2 record (Burckel et al., 2015) (Figures 3e and 3f) is coeval with Greenland Stadial 12 (Rasmussen et al., 2014), a stadial that is also related to an AMOC slowdown that was, however, weaker

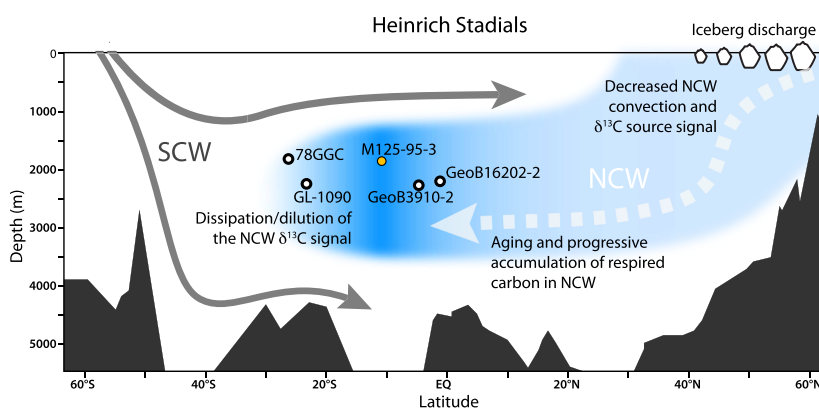


**Figure 5.** Schematic representation of the western Atlantic during Heinrich Stadials (i.e., under a weak Atlantic meridional overturning circulation). Arrows depict source region and the main pathway of the Southern Component Water (SCW) and Northern Component Water (NCW). NCW dashed arrow indicates decreased convection and aging of this water mass. Open and filled dots indicate core sites of GeoB16202-2 (western equatorial Atlantic) (Voigt et al., 2017), GeoB3910-2 (western equatorial Atlantic) (Burckel et al., 2015), M125-95-3 (western tropical South Atlantic) (this study), GL-1090 (western subtropical South Atlantic) (Santos et al., 2017), and 78GGC (western subtropical South Atlantic) (Tessin & Lund, 2013). The blue shading represents the magnitude of the NCW negative  $\delta^{13}\text{C}$  excursion (accumulation of respired carbon), which gradually increases southwards at mid-depth, peaking in the western tropical South Atlantic (i.e., M125-95-3 core site) from where it starts to dissipate/dilute by mixing with SCW toward the western subtropical South Atlantic (i.e., GL-1090 and 78GGC core sites).

ventilation, that is, bulk sediment S content, shows increases during all Heinrich Stadials of the last glacial and deglacial (exception made for the YD), indicating an increased residence time of NCW in the western tropical South Atlantic (Figures 2d, 2e, 3i, and 3j).

To our knowledge, the use of S to track millennial-scale changes in bottom water ventilation is unprecedented (Harff et al., 2011; Pasquier et al., 2017; Sluijs et al., 2008). Its use is grounded on the fact that an increase in the concentration of S at the seafloor is tightly related to local depletion in oxygen availability (Jørgensen et al., 2019; Jørgensen & Kasten, 2006). Since the flux of organic matter to the seafloor was low at our core site throughout the investigated period (Figures 2b and 2c), the S increases during Heinrich Stadials mainly reflect changes in oxygen availability of the bottom water (i.e., NCW). A reduced ventilation and accumulation of respiration carbon at NCW depths would decrease oxygen availability via aerobic organic matter degradation favoring the S accumulation at the seafloor (i.e., via sulfate-reducing bacteria anaerobic organic matter degradation). Despite the overall good similarity, our benthic  $\delta^{13}\text{C}$  and S records also show localized differences (e.g., during Heinrich Stadial 6). These localized differences most probably arise because of the partially different phenomena controlling both proxies.

The persistent negative  $\delta^{13}\text{C}$  excursions and positive S excursions during Heinrich Stadials of the last glacial and deglacial in our core (Figures 3f, 3i, and 3j) suggest that, even under different boundary conditions, similar mechanisms resulted in an increased NCW residence time and accumulation of respiration carbon in the western tropical South Atlantic mid-depth. Moreover, the synchronism between past increases in atmospheric CO<sub>2</sub> (CO<sub>2atm</sub>) (Ahn & Brook, 2008, 2014) and decreases in  $\delta^{13}\text{CO}_{2\text{atm}}$  (Bauska et al., 2018; Eggleston et al., 2016) during millennial-scale climate change events in the one hand and in the AMOC-related marine carbon cycle records on the other hand (Burckel et al., 2015; Santos et al., 2017; Tassin & Lund, 2013; Voigt et al., 2017) suggests that the AMOC played a relevant role in modulating the global carbon cycle during Heinrich Stadials.

#### Acknowledgments

Logistic and technical assistance was provided by the captain and crew of the R/V Meteor. New data shown herein are archived in Pangaea (doi: 10.1594/PANGAEA.915451). M. C. Campos acknowledges the financial support from Fundação de Amparo à Pesquisa do Estado de São Paulo (FAPESP) (Grants 2016/10242-0 and 2018/06790-7). C. M. Chiessi acknowledges the financial support from FAPESP (Grant 2018/15123-4), Coordenação de Aperfeiçoamento de Pessoal de Nível Superior (CAPES) (Grants 564/2015 and 88881.313535/2019-01), Conselho Nacional de Desenvolvimento Científico e Tecnológico (CNPq) (Grants 302607/2016-1 and 422255/2016-5), and the Alexander von Humboldt-Stiftung. CAPES (Grants 88887.156152/2017-00 and 88881.161151/2017-01) and CNPq (Grant 406322/2018-0) currently support I. M. Venancio. T. M. L. Pinho acknowledges the financial support from FAPESP (Grant 2019/10642-6). S. Crivellari acknowledges the financial support from CAPES (Grant 88887.196044/2018-00). A. L. S. Albuquerque is a senior CNPq researcher (Grants 302521-2017-8 and 429767/2018-8) and acknowledges the financial support from CAPES (Finance Code 001). S. Mulitza and H. Kuhnert were funded through the Deutsche Forschungsgemeinschaft (DFG) Research Centre, Cluster of Excellence "The Ocean in the Earth System". A. Bahr received funding from the DFG via Grant BA 3809/9-1.

## 6. Conclusions

We present new high-resolution  $\delta^{13}\text{C}$  and S records from the western tropical South Atlantic mid-depth for the last ca. 70 ka. This is the first western South Atlantic  $\delta^{13}\text{C}$  record that clearly registers all Heinrich Stadials of the last glacial and deglacial, filling the gap of shorter and lower temporal resolution marine records between 4.24°S and 24.92°S. The concurrent  $\delta^{13}\text{C}$  decreases and S increases during Heinrich Stadials in our records suggest reduced ventilation and consequent accumulation of respiration carbon at NCW depths. Based on the comparison of our new data to existing western South Atlantic marine records collected around the same water depth, we conclude that (i) even under different boundary conditions, negative  $\delta^{13}\text{C}$  excursions occurred during all Heinrich Stadials of the last glacial and deglacial, and (ii) the magnitude of the negative excursions suggests a coherent meridional pattern. This meridional pattern supports the notion that the Heinrich Stadials reduction in the NCW  $\delta^{13}\text{C}$  source signal together with the accumulation of respiration carbon at Atlantic NCW depths promoted a progressive depletion in the NCW  $\delta^{13}\text{C}$  signature along its southwards advection. The highest negative  $\delta^{13}\text{C}$  excursions occurred in the western tropical South Atlantic, from where the signal started to dissipate/dilute by mixing with SCW.

## References

- Ahn, J., & Brook, E. J. (2020). Atmospheric CO<sub>2</sub> and climate on millennial time scales during the last glacial period. *Science*, 322(5898), 83–85. <https://doi.org/10.1126/science.1160832>
- Ahn, J., & Brook, E. J. (2014). Siple Dome ice reveals two modes of millennial CO<sub>2</sub> change during the last ice age. *Nature Communications*, 5(1), 3723. <https://doi.org/10.1038/ncomms4723>
- Anderson, R. F., Ali, S., Bradtmiller, L. I., Nielsen, S. H., Fleisher, M. Q., Anderson, B. E., & Burckle, L. H. (2009). Wind-driven upwelling in the Southern Ocean and the deglacial rise in atmospheric CO<sub>2</sub>. *Science*, 323(5920), 1443–1448. <https://doi.org/10.1126/science.1167441>
- Bahr, A., Albuquerque, A. L. S., Ardenghi, N., Batenburg, S. J., Bayer, M., Catunda, M. C., et al. (2016). South American Hydrological Balance and Paleoceanography during the Late Pleistocene and Holocene (SAMBA) (4947148311550). Retrieved from [https://doi.org/10.2312/cr\\_m91](https://doi.org/10.2312/cr_m91)
- Bauska, T. K., Brook, E. J., Marcott, S., Baggenstos, D., Shackleton, S., Severinghaus, J., et al. (2018). Controls on millennial-scale atmospheric CO<sub>2</sub> variability during the last glacial period. *Geophysical Research Letters*, 45, 7731–7740. <https://doi.org/10.1029/2018GL077881>
- Bereiter, B., Lüthi, D., Siegrist, M., Schüpbach, S., Stocker, T. F., & Fischer, H. (2012). Mode change of millennial CO<sub>2</sub> variability during the last glacial cycle associated with a bipolar marine carbon seesaw. *Proceedings of the National Academy of Sciences*, 109(25), 9755–9760. <https://doi.org/10.1073/pnas.1204069109>

- Blaauw, M., & Christen, J. A. (2011). Flexible paleoclimate age-depth models using an autoregressive gamma process. *Bayesian Analysis*, 6(3), 457–474.
- Bolli, H. M., Saunders, J. B., & Perch-Nielsen, K. (1989). Plankton stratigraphy: Volume 1, Planktic foraminifera, calcareous nannofossils and calpionellids (Vol. 1). Cambridge: Cambridge University Press.
- Boltovskoy, E., Giussani, G., Watanabe, S., & Wright, R. (1980). *Atlas of benthic shelf foraminifera of the southwest Atlantic*. The Hague-Boston-London: Junk bv. Pub.
- Bottrell, S. H., & Newton, R. J. (2006). Reconstruction of changes in global sulfur cycling from marine sulfate isotopes. *Earth-Science Reviews*, 75(1–4), 59–83. <https://doi.org/10.1016/j.earscirev.2005.10.004>
- Boyle, E. A. (1990). Quaternary deepwater paleoceanography. *Science*, 249(4971), 863–870. <https://doi.org/10.1126/science.249.4971.863>
- Boyle, E. A., & Keigwin, L. (1987). North Atlantic thermohaline circulation during the past 20,000 years linked to high-latitude surface temperature. *Nature*, 330(6143), 35–40. <https://doi.org/10.1038/330035a0>
- Burckel, P., Waelbroeck, C., Gherardi, J. M., Pichat, S., Arz, H., Lippold, J., et al. (2015). Atlantic Ocean circulation changes preceded millennial tropical South America rainfall events during the last glacial. *Geophysical Research Letters*, 42, 411–418. <https://doi.org/10.1002/2014GL062512>
- Butzin, M., Köhler, P., & Lohmann, G. (2017). Marine radiocarbon reservoir age simulations for the past 50,000 years. *Geophysical Research Letters*, 44, 8473–8480. <https://doi.org/10.1002/2017GL074688>
- Campos, M. C., Chiessi, C. M., Prange, M., Mulitza, S., Kuhnert, H., Paul, A., et al. (2019). A new mechanism for millennial scale positive precipitation anomalies over tropical South America. *Quaternary Science Reviews*, 225, 105990. <https://doi.org/10.1016/j.quascirev.2019.105990>
- Chen, T., Robinson, L. F., Burke, A., Southon, J., Spooner, P., Morris, P. J., et al. (2015). Synchronous centennial abrupt events in the ocean and atmosphere during the last deglaciation. *Science*, 349(6255), 1537–1541. <https://doi.org/10.1126/science.aac6159>
- Curry, W., Marchitto, T., McManus, J., Oppo, D., & Laarkamp, K. (1999). *Millennial-scale changes in ventilation of the thermocline, intermediate, and deep waters of the glacial North Atlantic*, Geophysical Monograph, (Vol. 112, pp. 59–76). Washington, DC: American Geophysical Union.
- Dias, B. B., Barbosa, C. F., Faria, G. R., Seoane, J. C. S., & Albuquerque, A. L. S. (2018). The effects of multidecadal-scale phytopelotritus disturbances on the benthic foraminiferal community of a Western Boundary Upwelling System, Brazil. *Marine Micropaleontology*, 139, 102–112. <https://doi.org/10.1016/j.marmicro.2017.12.003>
- Duplessy, J., Shackleton, N., Fairbanks, R., Labeyrie, L., Oppo, D., & Kallel, N. (1988). Deepwater source variations during the last climatic cycle and their impact on the global deepwater circulation. *Paleoceanography*, 3(3), 343–360. <https://doi.org/10.1029/PA003i003p00343>
- Eggleson, S., Schmitt, J., Bereiter, B., Schneider, R., & Fischer, H. (2016). Evolution of the stable carbon isotope composition of atmospheric CO<sub>2</sub> over the last glacial cycle. *Paleoceanography*, 31, 434–452. <https://doi.org/10.1002/2015PA002874>
- Elliot, M., Labeyrie, L., & Duplessy, J.-C. (2002). Changes in North Atlantic deep-water formation associated with the Dansgaard–Oeschger temperature oscillations (60–10 ka). *Quaternary Science Reviews*, 21(10), 1153–1165. [https://doi.org/10.1016/S0277-3791\(01\)00137-8](https://doi.org/10.1016/S0277-3791(01)00137-8)
- Epica, C. M. (2006). One-to-one coupling of glacial climate variability in Greenland and Antarctica. *Nature*, 444(7116), 195–198. <https://doi.org/10.1038/nature05301>
- Fontanier, C., Jorissen, F., Licari, L., Alexandre, A., Anschutz, P., & Carbonel, P. (2002). Live benthic foraminiferal faunas from the Bay of Biscay: Faunal density, composition, and microhabitats. *Deep Sea Research Part I: Oceanographic Research Papers*, 49(4), 751–785. [https://doi.org/10.1016/S0967-0637\(01\)00078-4](https://doi.org/10.1016/S0967-0637(01)00078-4)
- Garcia, H. E., Locarnini, R. A., Boyer, T. P., Antonov, J. I., Baranova, O. K., Zweng, M. M., Reagan, J. R., & Johnson, D. R. (2013). World Ocean Atlas 2013. Vol. 4: Dissolved Inorganic Nutrients (phosphate, nitrate, silicate). S. Levitus & A. Mishonov NOAA *NESDIS* 76, (25). <https://doi.org/10.7289/V5J67DW>
- Govin, A., Chiessi, C. M., Zabel, M., Sawakuchi, A. O., Heslop, D., Hörner, T., et al. (2014). Terrigenous input off northern South America driven by changes in Amazonian climate and the North Brazil Current retroflection during the last 250 ka. *Climate of the Past*, 10(2), 843–862. <https://doi.org/10.5194/cp-10-843-2014>
- Harff, J., Endler, R., Emelyanov, E., Kotov, S., Leipe, T., Moros, M., et al. (2011). Late Quaternary climate variations reflected in Baltic Sea sediments. J. Harff S. Björck & P. Hoth In *The Baltic Sea basin*, Central and Eastern European Development Studies (CEEDES)3, 99–132. Berlin, Heidelberg: Springer. [https://doi.org/10.1007/978-3-642-17220-5\\_5](https://doi.org/10.1007/978-3-642-17220-5_5)
- Henry, L., McManus, J. F., Curry, W. B., Roberts, N. L., Piotrowski, A. M., & Keigwin, L. D. (2016). North Atlantic ocean circulation and abrupt climate change during the last glaciation. *Science*, 353(6298), 470–474. <https://doi.org/10.1126/science.aaf5529>
- Herguera, J. C., & Berger, W. (1991). Paleoproductivity from benthic foraminifera abundance: Glacial to postglacial change in the west-equatorial Pacific. *Geology*, 19(12), 1173–1176. [https://doi.org/10.1130/0091-7613\(1991\)019%3C:1173:PFBFAG%3E;2.3.CO;2](https://doi.org/10.1130/0091-7613(1991)019%3C:1173:PFBFAG%3E;2.3.CO;2)
- Howe, J. N., Huang, K.-F., Oppo, D. W., Chiessi, C. M., Mulitza, S., Bluszta, J., & Piotrowski, A. M. (2018). Similar mid-depth Atlantic water mass provenance during the Last Glacial Maximum and Heinrich Stadial 1. *Earth and Planetary Science Letters*, 490, 51–61. <https://doi.org/10.1016/j.epsl.2018.03.006>
- Jørgensen, B. B., Findlay, A. J., & Pellerin, A. (2019). The biogeochemical sulfur cycle of marine sediments. *Frontiers in Microbiology*, 10, 849–849. <https://doi.org/10.3389/fmicb.2019.00849>
- Jørgensen, B. B., & Kasten, S. (2006). Sulfur cycling and methane oxidation. H. D. Schulz & M. Zabel In *Marine geochemistry*, (pp. 271–309). Berlin, Heidelberg: Springer. [https://doi.org/10.1007/3-540-32144-6\\_8](https://doi.org/10.1007/3-540-32144-6_8)
- Keigwin, L. D., & Lehman, S. J. (1994). Deep circulation change linked to Heinrich event 1 and Younger Dryas in a middepth North Atlantic core. *Paleoceanography*, 9(2), 185–194. <https://doi.org/10.1029/94PA00032>
- Koho, K., García, R. D., De Stigter, H., Epping, E., Koning, E., Kouwenhoven, T., & Van der Zwaan, G. (2008). Sedimentary labile organic carbon and pore water redox control on species distribution of benthic foraminifera: A case study from Lisbon–Setúbal Canyon (southern Portugal). *Progress in Oceanography*, 79(1), 55–82. <https://doi.org/10.1016/j.pocean.2008.07.004>
- Kroopnick, P. (1985). The distribution of <sup>13</sup>C of ΣCO<sub>2</sub> in the world oceans. *Deep Sea Research Part A: Oceanographic Research Papers*, 32(1), 57–84. [https://doi.org/10.1016/0198-0149\(85\)90017-2](https://doi.org/10.1016/0198-0149(85)90017-2)
- Kucera, M., Weinelt, M., Kiefer, T., Pflaumann, U., Hayes, A., Weinelt, M., et al. (2005). Reconstruction of sea-surface temperatures from assemblages of planktonic foraminifera: Multi-technique approach based on geographically constrained calibration data sets and its application to glacial Atlantic and Pacific Oceans. *Quaternary Science Reviews*, 24(7–9), 951–998. <https://doi.org/10.1016/j.quascirev.2004.07.014>
- Langner, M., & Mulitza, S. (2019). PaleoDataView—A software toolbox for the collection, homogenization and visualization of marine proxy data. *Climate of the Past*, 15(6), 2067–2072. <https://doi.org/10.5194/cp-15-2067-2019>

- LeGrande, A. N., & Schmidt, G. A. (2006). Global gridded data set of the oxygen isotopic composition in seawater. *Geophysical Research Letters*, 33, L12604. <https://doi.org/10.1029/2006GL026011>
- Lisiecki, L. E., & Stern, J. V. (2016). Regional and global benthic  $\delta^{18}\text{O}$  stacks for the last glacial cycle. *Paleoceanography*, 31, 1368–1394. <https://doi.org/10.1002/2016PA003002>
- Lund, D., Tessin, A., Hoffman, J., & Schmittner, A. (2015). Southwest Atlantic water mass evolution during the last deglaciation. *Paleoceanography*, 30, 477–494. <https://doi.org/10.1002/2014PA002657>
- Lutze, G. F. (1986). *Uvigerina* species of the eastern North Atlantic. In G. J. van der Zwaan, F. J. Jorissen, P. J. J. M. Verhallen, & C. H. Von Daniels (Eds.), *Atlantic-European Oligocene to recent Uvigerina: Taxonomy, paleoecology and paleobiogeography, Utrecht Micropaleontological Bulletins*, (Vol. 35, pp. 21–46). Utrecht University.
- Lynch-Stieglitz, J., Schmidt, M. W., Henry, L. G., Curry, W. B., Skinner, L. C., Multizzi, S., et al. (2014). Muted change in Atlantic overturning circulation over some glacial-aged Heinrich events. *Nature Geoscience*, 7(2), 144–150. <https://doi.org/10.1038/ngeo2045>
- Lynch-Stieglitz, J., Stocker, T. F., Broecker, W. S., & Fairbanks, R. G. (1995). The influence of air-sea exchange on the isotopic composition of oceanic carbon: Observations and modeling. *Global Biogeochemical Cycles*, 9(4), 653–665. <https://doi.org/10.1029/95GB02574>
- Mackensen, A., Hubberten, H. W., Bickert, T., Fischer, G., & Fütterer, D. (1993). The  $\delta^{13}\text{C}$  in benthic foraminiferal tests of *Fontbotia wuellerstorfi* (Schwager) relative to the  $\delta^{13}\text{C}$  of dissolved inorganic carbon in Southern Ocean Deep Water: Implications for glacial ocean circulation models. *Paleoceanography*, 8(5), 587–610. <https://doi.org/10.1029/93PA01291>
- Mackensen, A., & Schmiedl, G. (2019). Stable carbon isotopes in paleoceanography: Atmosphere, oceans, and sediments. *Earth-Science Reviews*, 102893.
- McCorkle, D. C., Emerson, S. R., & Quay, P. D. (1985). Stable carbon isotopes in marine porewaters. *Earth and Planetary Science Letters*, 74(1), 13–26. [https://doi.org/10.1016/0012-821X\(85\)90162-1](https://doi.org/10.1016/0012-821X(85)90162-1)
- McCorkle, D. C., Keigwin, L. D., Corliss, B. H., & Emerson, S. R. (1990). The influence of microhabitats on the carbon isotopic composition of deep-sea benthic foraminifera. *Paleoceanography*, 5(2), 161–185. <https://doi.org/10.1029/PA005i002p00161>
- McManus, J. F., Francois, R., Gherardi, J.-M., Keigwin, L. D., & Brown-Leger, S. (2004). Collapse and rapid resumption of Atlantic meridional circulation linked to deglacial climate changes. *Nature*, 428(6985), 834–837. <https://doi.org/10.1038/nature02494>
- Meckler, A., Sigman, D. M., Gibson, K., Francois, R., Martinez-Garcia, A., Jaccard, S., et al. (2013). Deglacial pulses of deep-ocean silicate into the subtropical North Atlantic Ocean. *Nature*, 495(7442), 495–498. <https://doi.org/10.1038/nature12006>
- Meredith, M. P., Heywood, K. J., Frew, R. D., & Dennis, P. F. (1999). Formation and circulation of the water masses between the southern Indian Ocean and Antarctica: Results from  $\delta^{18}\text{O}$ . *Journal of Marine Research*, 57(3), 449–470. <https://doi.org/10.1357/002224099764805156>
- Milzer, G., Giraudeau, J., Rühlemann, C., Faust, J., Knies, J., & Schmidt, S. (2016). Benthic stable isotope variability in the Trondheimsfjord during the last 50 years: Proxy records of mixing dynamics related to NAO. *Estuarine, Coastal and Shelf Science*, 172, 34–46. <https://doi.org/10.1016/j.ecss.2016.01.034>
- Multizzi, S., Chiessi, C. M., Schefuß, E., Lippold, J., Wichmann, D., Antz, B., et al. (2017). Synchronous and proportional deglacial changes in Atlantic meridional overturning and northeast Brazilian precipitation. *Paleoceanography*, 32, 622–633. <https://doi.org/10.1002/2017PA003084>
- Oppo, D. W., Curry, W. B., & McManus, J. F. (2015). What do benthic  $\delta^{13}\text{C}$  and  $\delta^{18}\text{O}$  data tell us about Atlantic circulation during Heinrich Stadial 1? *Paleoceanography*, 30, 353–368. <https://doi.org/10.1002/2014PA002667>
- Oppo, D. W., & Fairbanks, R. G. (1987). Variability in the deep and intermediate water circulation of the Atlantic Ocean during the past 25,000 years: Northern Hemisphere modulation of the Southern Ocean. *Earth and Planetary Science Letters*, 86(1), 1–15. [https://doi.org/10.1016/0012-821X\(87\)90183-X](https://doi.org/10.1016/0012-821X(87)90183-X)
- Pasquier, V., Sansjofre, P., Rabineau, M., Revillon, S., Houghton, J., & Fike, D. A. (2017). Pyrite sulfur isotopes reveal glacial–interglacial environmental changes. *Proceedings of the National Academy of Sciences*, 114(23), 5941–5945. <https://doi.org/10.1073/pnas.1618245114>
- Patterson, R. T., & Fishbein, E. (1989). Re-examination of the statistical methods used to determine the number of point counts needed for micropaleontological quantitative research. *Journal of Paleontology*, 63(2), 245–248. <https://doi.org/10.1017/S002233600019272>
- Polyak, L., Stanovoy, V., & Lubinski, D. J. (2003). Stable isotopes in benthic foraminiferal calcite from a river-influenced Arctic marine environment, Kara and Pechora Seas. *Paleoceanography*, 18(1), 1003. <https://doi.org/10.1029/2001PA000752>
- Portillo-Ramos, R., Chiessi, C., Zhang, Y., Multizzi, S., Kucera, M., Siccha, M., et al. (2017). Coupling of equatorial Atlantic surface stratification to glacial shifts in the tropical rainbelt. *Scientific Reports*, 7(1), 1561. <https://doi.org/10.1038/s41598-017-01629-z>
- Rasmussen, S. O., Bigler, M., Blockley, S. P., Blunier, T., Buchardt, S. L., Clausen, H. B., et al. (2014). A stratigraphic framework for abrupt climatic changes during the Last Glacial period based on three synchronized Greenland ice-core records: Refining and extending the INTIMATE event stratigraphy. *Quaternary Science Reviews*, 106, 14–28. <https://doi.org/10.1016/j.quascirev.2014.09.007>
- Reimer, P. J., Bard, E., Bayliss, A., Beck, J. W., Blackwell, P. G., Ramsey, C. B., et al. (2013). IntCal13 and Marine13 radiocarbon age calibration curves 0–50,000 years cal BP. *Radiocarbon*, 55(4), 1869–1887, DOI: [https://doi.org/10.2458/azu\\_js\\_rc.55.16947](https://doi.org/10.2458/azu_js_rc.55.16947)
- Rhein, M., Stramma, L., & Send, U. (1995). The Atlantic deep western boundary current: Water masses and transports near the equator. *Journal of Geophysical Research*, 100(C2), 2441–2457. <https://doi.org/10.1029/94JC02355>
- Robinson, L. F., Adkins, J. F., Keigwin, L. D., Southon, J., Fernandez, D. P., Wang, S., & Scheirer, D. S. (2005). Radiocarbon variability in the western North Atlantic during the last deglaciation. *Science*, 310(5753), 1469–1473. <https://doi.org/10.1126/science.1114832>
- Santos, T. P., Lessa, D. O., Venancio, I. M., Chiessi, C. M., Multizzi, S., Kuhnhert, H., et al. (2017). Prolonged warming of the Brazil Current precedes deglaciations. *Earth and Planetary Science Letters*, 463, 1–12. <https://doi.org/10.1016/j.epsl.2017.01.014>
- Sarmiento, J., Toggweiler, J., & Najjar, R. (1988). Ocean carbon-cycle dynamics and atmospheric  $\text{pCO}_2$ . *Philosophical Transactions of the Royal Society of London. Series A, Mathematical and Physical Sciences*, 325(1583), 3–21.
- Sarnthein, M., Winn, K., Jung, S. J., Duplessy, J. C., Labeyrie, L., Erlenkeuser, H., & Ganssen, G. (1994). Changes in east Atlantic deepwater circulation over the last 30,000 years: Eight time slice reconstructions. *Paleoceanography*, 9(2), 209–267. <https://doi.org/10.1029/93PA03301>
- Schliman, B., Almogi-Labin, A., Bar-Matthews, M., Labeyrie, L., Paterné, M., & Luz, B. (2001). Long-and short-term carbon fluctuations in the Eastern Mediterranean during the late Holocene. *Geology*, 29(12), 1099–1102. [https://doi.org/10.1130/0091-7613\(2001\)029%3C1099:LASTCF%3E;2.0.CO;2](https://doi.org/10.1130/0091-7613(2001)029%3C1099:LASTCF%3E;2.0.CO;2)
- Schlitzer, R. (2018). Ocean Data View, <https://odv.awi.de>
- Schmiedl, G., De Bovée, F., Buscail, R., Charrière, B., Hemleben, C., Medernach, L., & Picon, P. (2000). Trophic control of benthic foraminiferal abundance and microhabitat in the bathyal Gulf of Lions, western Mediterranean Sea. *Marine Micropaleontology*, 40(3), 167–188. [https://doi.org/10.1016/S0377-8398\(00\)00038-4](https://doi.org/10.1016/S0377-8398(00)00038-4)

- Schmiedl, G., & Mackensen, A. (1997). Late Quaternary paleoproductivity and deep water circulation in the eastern South Atlantic Ocean: Evidence from benthic foraminifera. *Paleogeography, Palaeoclimatology, Palaeoecology*, 130(1–4), 43–80. [https://doi.org/10.1016/S0031-0182\(96\)00137-X](https://doi.org/10.1016/S0031-0182(96)00137-X)
- Schmiedl, G., & Mackensen, A. (2006). Multispecies stable isotopes of benthic foraminifers reveal past changes of organic matter decomposition and deepwater oxygenation in the Arabian Sea. *Paleoceanography*, 21, PA4213. <https://doi.org/10.1029/2006PA001284>
- Schmiedl, G., Pfeilsticker, M., Hemleben, C., & Mackensen, A. (2004). Environmental and biological effects on the stable isotope composition of recent deep-sea benthic foraminifera from the western Mediterranean Sea. *Marine Micropaleontology*, 51(1–2), 129–152. <https://doi.org/10.1016/j.marmicro.2003.10.001>
- Schmittner, A., & Lund, D. (2015). Early deglacial Atlantic overturning decline and its role in atmospheric CO<sub>2</sub> rise inferred from carbon isotopes ( $\delta^{13}\text{C}$ ). *Climate of the Past*, 11(2), 135–152. <https://doi.org/10.5194/cp-11-135-2015>
- Schrag, D. P., Adkins, J. F., McIntyre, K., Alexander, J. L., Hodell, D. A., Charles, C. D., & McManus, J. F. (2002). The oxygen isotopic composition of seawater during the Last Glacial Maximum. *Quaternary Science Reviews*, 21(1–3), 331–342. [https://doi.org/10.1016/S0277-3791\(01\)00110-X](https://doi.org/10.1016/S0277-3791(01)00110-X)
- Shackleton, N. J., & Hall, M. A. (1984). Oxygen and carbon isotope stratigraphy of DSDP Hole 552A: Plio-Pleistocene glacial history. *Initial Reports of the Deep Sea Drilling Project*, 81, 599–609.
- Skinner, L., & Shackleton, N. (2005). An Atlantic lead over Pacific deep-water change across Termination I: Implications for the application of the marine isotope stage stratigraphy. *Quaternary Science Reviews*, 24(5–6), 571–580. <https://doi.org/10.1016/j.quascirev.2004.11.008>
- Sluijs, A., Röhl, U., Schouten, S., Brumsack, H. J., Sangiorgi, F., Damsté, J. S. S., & Brinkhuis, H. (2008). Arctic late Paleocene–early Eocene paleoenvironments with special emphasis on the Paleocene–Eocene thermal maximum (Lomonosov Ridge, Integrated Ocean Drilling Program Expedition 302). *Paleoceanography*, 23, PA1S11. <https://doi.org/10.1029/2007PA001495>
- Stainforth, R., Lamb, J. L., Luterbacher, H., Beard, J. H., & Jeffords, R. M. (1975). Cenozoic planktonic foraminiferal zonation and characteristics of index forms. University of Kansas Paleontological Contributions, Article 62, 162 pp.
- Stramma, L., & England, M. (1999). On the water masses and mean circulation of the South Atlantic Ocean. *Journal of Geophysical Research*, 104(C9), 20,863–20,883. <https://doi.org/10.1029/1999JC900139>
- Stuiver, M., Quay, P. D., & Ostlund, H. (1983). Abyssal water carbon-14 distribution and the age of the world oceans. *Science*, 219(4586), 849–851. <https://doi.org/10.1126/science.219.4586.849>
- Süfke, F., Pöppelmeier, F., Goepfert, T. J., Regelous, M., Koutsodendris, A., Blaser, P., et al. (2019). Constraints on the northwestern Atlantic deep water circulation from  $^{231}\text{Pa}/^{230}\text{Th}$  during the last 30,000 years. *Paleoceanography and Paleoclimatology*, 34, 1945–1958. <https://doi.org/10.1029/2019PA003737>
- Suits, N. S., & Arthur, M. A. (2000). Sulfur diagenesis and partitioning in Holocene Peru shelf and upper slope sediments. *Chemical Geology*, 163(1–4), 219–234. [https://doi.org/10.1016/S0009-2541\(99\)00114-X](https://doi.org/10.1016/S0009-2541(99)00114-X)
- Tessin, A., & Lund, D. (2013). Isotopically depleted carbon in the mid-depth South Atlantic during the last deglaciation. *Paleoceanography*, 28, 296–306. <https://doi.org/10.1002/palo.20026>
- Theodor, M., Schmiedl, G., Jorissen, F., & Mackensen, A. (2016). Stable carbon isotope gradients in benthic foraminifera as proxy for organic carbon fluxes in the Mediterranean Sea. *Biogeosciences*, 13(23), 6385–6404. <https://doi.org/10.5194/bg-13-6385-2016>
- Thornalley, D. J., Barker, S., Broecker, W. S., Elderfield, H., & McCave, I. N. (2011). The deglacial evolution of North Atlantic deep convection. *Science*, 331(6014), 202–205.
- Voigt, I., Cruz, A., Mulitza, S., Chiessi, C., Mackensen, A., Lippold, J., et al. (2017). Variability in mid-depth ventilation of the western Atlantic Ocean during the last deglaciation. *Paleoceanography*, 32, 948–965. <https://doi.org/10.1002/2017PA003095>
- Volbers, A., & Henrich, R. (2004). Calcium carbonate corrosiveness in the South Atlantic during the Last Glacial Maximum as inferred from changes in the preservation of *Globigerina bulloides*: A proxy to determine deep-water circulation patterns? *Marine Geology*, 204(1–2), 43–57. [https://doi.org/10.1016/S0025-3227\(03\)00372-4](https://doi.org/10.1016/S0025-3227(03)00372-4)
- Waelbroeck, C., Labeyrie, L., Michel, E., Duplessy, J. C., McManus, J. F., Lambeck, K., et al. (2002). Sea-level and deep water temperature changes derived from benthic foraminifera isotopic records. *Quaternary Science Reviews*, 21(1–3), 295–305. [https://doi.org/10.1016/S0277-3791\(01\)00101-9](https://doi.org/10.1016/S0277-3791(01)00101-9)
- Waelbroeck, C., Skinner, L. C., Labeyrie, L., Duplessy, J. C., Michel, E., Vazquez Riveiros, N., et al. (2011). The timing of deglacial circulation changes in the Atlantic. *Paleoceanography*, 26, PA3213. <https://doi.org/10.1029/2010PA002007>
- Zahn, R., Schönfeld, J., Kudrass, H., Park, M., Erlenkeuser, H., & Grootes, P. (1997). Thermohaline instability in the North Atlantic during meltwater events: Stable isotope and ice-raftered detritus records from Core SO75-26KL, Portuguese Margin. *Paleoceanography*, 12(5), 696–710. <https://doi.org/10.1029/97PA00581>
- Zahn, R., Winn, K., & Samthein, M. (1986). Benthic foraminiferal  $\delta^{13}\text{C}$  and accumulation rates of organic carbon: *Uvigerina peregrina* group and *Cibicidoides wuellerstorfi*. *Paleoceanography*, 1(1), 27–42. <https://doi.org/10.1029/PA001i001p00027>
- Zhao, N., Oppo, D. W., Huang, K.-F., Howe, J. N., Blusztajn, J., & Keigwin, L. D. (2019). Glacial–interglacial Nd isotope variability of North Atlantic Deep Water modulated by North American ice sheet. *Nature Communications*, 10(1), 1–10.